Society For Biomaterials

Influence of PDLA nanoparticles size on drug release and interaction with cells

Ana Luísa Cartaxo,[1,2] Ana R. Costa-Pinto,[3] Albino Martins,[1,2] Susana Faria,[4] Virgínia M. F. Gonçalves,[5] Maria Elizabeth Tiritan,[5,6,7] Helena Ferreira,[1,2] Nuno M. Neves[1,2,8]

[1]3B's Research Group, I3Bs – Research Institute on Biomaterials, Biodegradables and Biomimetics, University of Minho, Headquarters of the European Institute of Excellence on Tissue Engineering and Regenerative Medicine, Guimarães, Portugal
[2]ICVS/3B's – PT Government Associate Laboratory, Braga, Portugal
[3]Universidade Católica Portuguesa, CBQF – Centro de Biotecnologia e Química Fina – Laboratório Associado, Escola Superior de Biotecnologia, 4200-374, Porto, Portugal
[4]Department of Mathematics for Science and Technology, Research CMAT, University of Minho, 4800-058, Guimarães, Portugal
[5]CESPU, Instituto de Investigação e Formação Avançada em Ciências e Tecnologias da Saúde, Paredes, Portugal
[6]Laboratório de Química Orgânica e Farmacêutica, Departamento de Ciências Químicas, Faculdade de Farmácia, Universidade do Porto, 4050-313, Porto, Portugal
[7]Centro Interdisciplinar de Investigação Marinha e Ambiental (CIIMAR/CIMAR), Universidade do Porto, 4050-123, Porto, Portugal
[8]The Discoveries Centre for Regenerative and Precision Medicine, Headquarters at University of Minho, Guimarães, Portugal

Received 2 January 2018; revised 1 October 2018; accepted 8 October 2018
Published online 00 Month 2018 in Wiley Online Library (wileyonlinelibrary.com). DOI: 10.1002/jbm.a.36563

Abstract: Polymeric nanoparticles (NPs) are strong candidates for the development of systemic and targeted drug delivery applications. Their size is a determinant property since it defines the NP–cell interactions, drug loading capacity, and release kinetics. Herein, poly(D,L-lactic acid) (PDLA) NPs were produced by the nanoprecipitation method, in which the influence of type and concentration of surfactant as well as PDLA concentration were assessed. The adjustment of these parameters allowed the successful production of NPs with defined medium sizes, ranging from 80 to 460 nm. The surface charge of the different NPs populations was consistently negative. Prednisolone was effectively entrapped and released from NPs with statistically different medium sizes (i.e., 80 or 120 nm). Release profiles indicate that these systems were able to deliver appropriate amounts of drug with potential applicability in the treatment of inflammatory conditions. Both NPs populations were cytocompatible with human endothelial and fibroblastic cells, in the range of concentrations tested (0.187–0.784 mg/mL). However, confocal microscopy revealed that within the range of sizes tested in our experiments, NPs presenting a medium size of 120 nm were able to be internalized in endothelial cells. In summary, this study demonstrates the optimization of the processing conditions to obtain PDLA NPs with narrow size ranges, and with promising performance for the treatment of inflammatory diseases. © 2018 Wiley Periodicals, Inc. J Biomed Mater Res Part A: 00A: 000–000, 2018.

Key Words: PDLA nanoparticles, size distribution, prednisolone, cytocompatibility, cell internalization

How to cite this article: Cartaxo AL, Costa-Pinto AR, Martins A, Faria S, Gonçalves Virgínia M. F., Tiritan ME, Ferreira H, Neves NM. 2018. Influence of PDLA nanoparticles size on drug release and interaction with cells. J Biomed Mater Res Part A. 2018:9999:1–12.

INTRODUCTION

Biomaterials structuring at a micro- and nano-scale are subject of considerable research due to their potential to improve the safety and efficacy of currently available therapies. Indeed, the use of these structured biomaterials as delivery devices allows surpassing solubility problems of the therapeutic agents, leading to reduced systemic toxicity and tissue damage.[1] Additionally, they can be designed to protect drugs, peptides, proteins and nucleic acids from premature degradation and undesirable interactions with the biological environment, preserving its bioavailability for longer periods of time.[2–5] The undesirable side effects in surrounding healthy tissues, due to drug distribution throughout the entire organism, can also be circumvented by delivering therapeutic agents into a specific organ or tissue, using antibodies, peptides or other targeting moieties linked to the surface of the delivery devices.[6–9]

Nanoparticles (NPs; 1–1000 nm) have specific advantages with respect to microparticles (MPs; 1–1000 μm),

Additional Supporting Information may be found in the online version of this article.
Correspondence to: N. M. Neves; e-mail: nuno@i3bs.uminho.pt.
Contract grant sponsor: QREN project "RL2-SCN-NORTE-07-0124-FEDER-000018" co-financed by the North Portugal Regional Operational Program (ON.2, O Novo Norte) under the NSRF through the ERDF
Contract grant sponsor: Portuguese Foundation for Science and Technology; contract grant number: SFRH/BPD/38939/2007 and SFRH/BPD/90332/2012

particularly when they need to target defined cells/tissues, after systemic administration.[10] Due to their size, NPs have a higher specific surface area than MPs,[11] which allows a faster drug release,[12,13] specifically when diffusion is the main release mechanism. Moreover, NPs are internalized by cells 15–250 times more than MPs in the 1–10 μm range,[14] which is an essential parameter when an intracellular action is required. Among all types of NPs,[15–19] polymeric ones fulfill a wide range of requirements to be used as delivery devices of therapeutic agents: (i) their size can be tailored to achieve specific biologic actions; (ii) they allow the stabilization of labile compounds; (iii) the release of loaded drugs can be controlled by fine-tuning the polymer characteristics; (iv) they can present a high stability, and (v) their surface can be easily modified.[20,21] Polymers of different origins have been proposed to produce NPs for drug delivery, ranging from natural-origin such as chitosan,[22,23] alginate,[24] gelatin, or albumin,[25,26] to synthetic-origin like poly(lactic acid) (PLA), poly(glycolic acid) (PGA) or poly(lactide-*co*-glycolide) (PLGA). These synthetic polymers are biodegradable aliphatic polyesters and, due to their non-toxicity and biocompatibility, have been already proposed for medical applications.[27–29] Between the previously referred biodegradable aliphatic polyesters, PLA, and more precisely PDLA, was chosen to be used in this work due to its slow degradation rate,[30] which can be advantageous if a sustained drug release is desired.

In this work, prednisolone was used as a drug model to be encapsulated inside PDLA NPs, since this bioactive compound is a broadly used glucocorticoid in the treatment of a wide range of inflammatory conditions.[31] However, its conventional administration leads to several adverse effects, such as osteoporosis, myopathy, and glaucoma.[32,33] Therefore, the incorporation of this glucocorticoid into a delivery device will allow improving its pharmacokinetic and pharmacodynamic, and, consequently, increase its therapeutic index and patient compliance.

Nanoparticles are potential tools to intracellularly deliver therapeutic agents, such as antiretroviral microbicides [34] and antituberculosis drugs,[35] in different cell types.[36,37] Therefore, to assess the potential of the developed NPs as intracellular drug delivery devices without specific surface functionalization (e.g., with antibodies to increase the internalization rate),[38–40] both endothelial and fibroblastic cells were used, to envisage different possible interactions of the NPs with specific tissues. Endothelial cells are, for example, key targets in vascular inflammation and, consequently, in vascular diseases, such as atherosclerosis,[41] whereas fibroblastic cells can be strategic therapeutic targets to treat chronic inflammatory conditions (e.g., rheumatoid arthritis).[42]

The main rationale of this work was to produce PDLA NPs with a confined size range, an efficient drug release profile and cell internalization ability to treat inflammatory diseases. Therefore, PDLA NPs were prepared by an optimization of the nanoprecipitation method, using different quantities of surfactant or organic/aqueous (org/aq) volume ratios. Size distribution and surface electrical charge were assessed, as well as morphology and storage stability of the developed PDLA NPs. Loading and entrapment efficiencies of prednisolone and its *in vitro* release profile were also evaluated. Cytocompatibility studies were performed with human endothelial and fibroblastic cells by assessing their viability, proliferation, and total protein content, as well as cell internalization of PDLA NPs (Scheme 1).

MATERIALS AND METHODS

Reagents

Chemical reagents, unless otherwise noted, were purchased from Sigma-Aldrich. Poly(D,L-lactic acid) (PDLA 02, MW 17 kg/mol) was kindly provided by Purasorb. Acetone (min. 99.8%) was purchased from Analar Normapur and acetonitrile (HPLC grade) was purchased from Fisher Scientific. Dubbelco's modified eagle's medium (DMEM), low glucose DMEM without phenol red and M199 medium were purchased to Sigma-Aldrich. Fetal bovine serum (FBS), Glutamax, antibiotic/antimycotic solution (10,000 units/mL penicillin G sodium, 10,000 μg/mL streptomycin sulfate, and

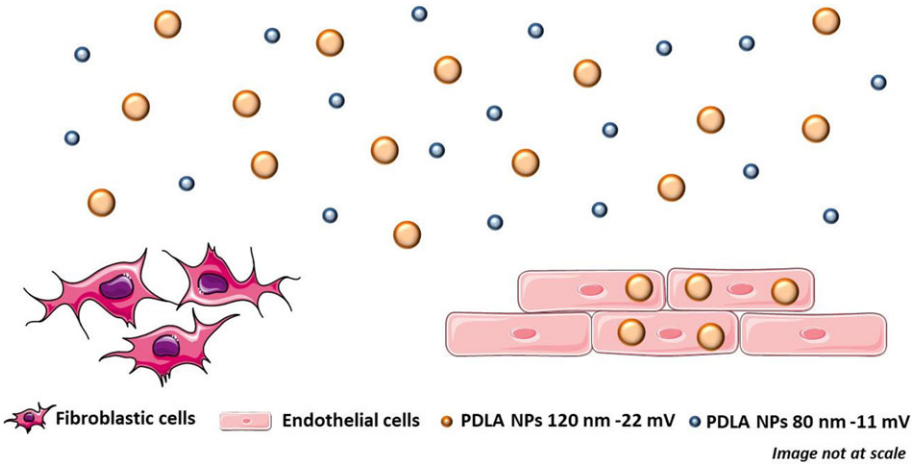

SCHEME 1. Schematic illustration of the interaction of the PDLA NPs presenting approximately 80 or 120 nm of size with fibroblasts and endothelial cells.

25 μg/mL amphotericin B), trypLE Express and Quant-iT™ PicoGreen® dsDNA Kit were purchased to Life Technologies. Endothelial cell growth supplement (ECGS) was purchased from Corning. CellTiter 96 AQueous One Solution kit was purchased from Promega, whereas the Micro BCA™ Protein Assay Kit was purchased from TermoFisher Scientific. Distilled and ultrapure water was obtained from MiliQ-Pore. All reagents were laboratory grade and were used as received.

NPs preparation

NPs were produced by the nanoprecipitation method, using two different processing conditions. The first condition was adapted from the literature,[34–37] with some modifications (Supporting Information Fig. S1), and was optimized to obtain NPs with reproducible size distribution. Briefly, an organic solution was prepared by dissolving PDLA (1.85 mg/mL) in acetone (5 mL), at room temperature (RT). Then, this mixture was added dropwise onto an aqueous solution (5 mL), under constant magnetic stirring, containing or not a hydrophilic surfactant (Pluronic® F-68) at different concentrations (0.10; 0.25; 0.50; 0.75; 1; 2; 3, or 5% v/v). After stirring the solution during 5 min, the organic solvent was removed under reduced pressure (3–8 mbar). For drug loading and release experiments, 3 mg of prednisolone was added to the initial organic solution. For fluorescence biological assays, 100 μL of fluorescein isothiocyanate (FITC) (1 mg/mL in ethanol) was added to the aqueous solution. Non-incorporated compounds were eliminated by centrifugation (two cycles of 45 min, 4000 rpm at 25°C) using Amicon Ultra-15 Centrifugal Filter Units. Before centrifugation, glucose (1 mg/mL) was added to avoid NPs aggregation.[43]

The second condition was designed to obtain NPs with a smaller size, as adapted from the literature[44] (Supporting Information Fig. S2). Briefly, an organic solution containing the same polymer, but in different concentration (0.37 mg/mL), was added to an aqueous solution containing or not a surfactant. In this method, different org/aq volume ratios (1:2, 1:3, 1:4, 1:5, 1:8, 1:10, and 1:15) were used. NPs preparation and labeling with FITC were performed as described above. For drug loading experiments, the protocol was also referred above, but instead of 3 mg, 1.5 mg of prednisolone was added to the PDLA solution.

Independently of the production method, all NPs suspensions were kept at 4°C under static conditions until further analysis.

NPs size, PDI, and zeta potential

Size and polydispersity index (PDI) were assessed by dynamic light scattering (DLS), and zeta potential by laser Doppler micro-electrophoresis in a Zetasizer ZS equipment (Malvern Instruments). The determinations were performed at 25°C using samples diluted in distilled water (1:50 v/v). The reported values are the average of three different measurements of, at least, three NPs populations prepared independently (n = 3).

NPs morphology

Morphological analyzes were conducted using atomic force microscopy (AFM; Dimension icon, BRUKER – tips Scanasyst Air). Prior to AFM analyzes, samples were diluted to achieve a final concentration of 0.1 mg/mL and disposed at the surface of a glass slide.

Long-term NPs stability

Storage stability of NPs suspensions was assessed by evaluating their size, PDI and zeta potential, as well as by observing their macroscopic sedimentation. NPs were kept in water at 4°C under static conditions, during the experimental period (6 months). At each time point, a sample dilution was prepared and measured, as explained before.

Drug entrapment efficiency and loading

After the production of NPs incorporating prednisolone, the resulting suspension was centrifuged to ensure that all non-incorporated drug was removed, as just referred. Then, prednisolone entrapped into NPs was quantified by high performance liquid chromatography (HPLC). A Shimadzu UFLC Prominence system equipped with two pumps LC-20 AD, an autosampler SIL-20 AC, a column oven CTO-20 AC, a degasser DGU-20A5, a system controller CBM-20A and a LC solution, version 1.24 SP1 (Shimadzu Corporation) were used. A Shimadzu SPD-20A UV/Vis detector was coupled to the LC system, with the wavelength set at 244 nm. A guard column LiChrocart® LiChrospher 100 RP-18 (4 × 4 mm, 5 μm; Merck) was connected to a Lichrocart® LiChrospher 100 RP-18 (250 × 4.6 mm; 5 mm; Merck) column. The mobile phase was composed by ultrapure water/acetonitrile (60:40, v/v), at isocratic mode (1 mL/min). The injection volume of each sample/standard was 20 μL. The specificity of the method was confirmed by comparing the chromatograms of standards with those of empty NPs.

Based on the results obtained by HPLC, drug entrapment efficiency and drug loading parameters were calculated by using the following equations:

$$\text{Entrapment efficiency}\,(\%) = \frac{\text{Prednisolone mass in NPs}}{\text{Initial prednisolone mass}} \times 100 \quad (1)$$

$$\text{Drug loading}\,(\%) = \frac{\text{Loaded prednisolone mass}}{\text{Total NPs mass}} \times 100 \quad (2)$$

The mass of prednisolone in NPs suspensions was obtained based on the peak areas of the chromatograms (acquired in triplicate). Previously, a prednisolone calibration curve was elaborated using acetonitrile as diluent, as for the tested samples.

In vitro drug release profile

The release of prednisolone from PDLA NPs was assessed using a dialysis cellulose tube (14.000 MWCO, Sigma-Aldrich) as the exclusive physical barrier. The dialysis

cellulose tubes were immersed in water for 20 min at RT and, then, washed thoroughly with ultrapure water. After removing the non-incorporated drug, NPs suspesions were suspended in phosphate buffer saline (PBS) (pH = 7.4, 0.01*M*) and then introduced into the dialysis tubes. These tubes containing NPs suspensions were kept in PBS at 37°C, under constant stirring. At each time point, samples of the surrounding solution were collected to determine the amount of prednisolone released from the NPs. An equal quantity of fresh PBS was added to maintain the initial releasing volume. The collected samples were diluted with acetonitrile and analyzed by HPLC, under the previously referred conditions.

Cell culture

Human microvascular endothelial (HPMECST1.6R) and fibroblastic (MRC-5) cell lines, both from pulmonary origin, were used to assess the cytocompatibility and internalization of PDLA NPs. Endothelial cells were cultured in M199 medium supplemented with 20% FBS, 2 m*M* Glutamax, 1% pen/strep (100 U/100 μg/mL) and ECGS (50 μg/mL). MRC-5 cells were cultured in DMEM supplemented with 10% FBS and 1% pen/strep (100 U/100 μg/mL). Culture medium was changed twice a week and cells were split when 90% of confluence was reached. Cells were incubated at 37°C in a humidified 5% CO_2 atmosphere. HPMECST1.6R cells were used at passages 32–34 and MRC-5 cells at passages 13–15.

NPs cytocompatibility assay

For both selected formulations, 1:10, 1:5, and 1:2.5 dilutions of the original suspension of PDLA NPs (0.187, 0.374, and 0.748 mg/mL, respectively) were prepared to perform biological assays. NPs suspensions were filtered through 0.22 μm filters (TPP) to ensure sterility.

Cells were harvested and seeded at the bottom of 24 wells plates using 100,000 cells per well. After 24 h, culture medium was removed and wells were washed with PBS and new culture medium containing different concentrations of NPs was added. Cells cultured without NPs (only with culture medium) were used as controls (CTRL). After 24, 48, and 72 h of culture, samples were collected to evaluate cell viability (MTS), proliferation (DNA) and total protein quantification.

Cell viability. The metabolic activity of the cells treated or not with different PDLA NPs concentrations was determined by MTS assay (CellTiter 96® AQueous One Solution). Briefly, culture medium without FBS and phenol red was mixed with MTS reagent (5:1 volume ratio) and added to each condition (n = 3). Samples were incubated for 3 h at 37°C, in a humidified 5% CO_2 atmosphere. The absorbance of each well (96-well plate) was read in triplicate at 490 nm, using a microplate reader (Synergy HT, Bio-TEK).

Cell proliferation. Cell proliferation was determined using a fluorimetric dsDNA quantification kit (Quant-iT™ PicoGreen®; Molecular Probes). Cells were transferred to eppendorf tubes containing 1 mL of ultrapure water and frozen at −80°C until further analysis. Prior to DNA quantification, cells were thawed and sonicated for 10 min. DNA standards were prepared at concentrations ranging from 0 to 1.5 μg/mL. To each well of an opaque 96-well plate (Falcon) were added 28.8 μL of sample or standard (n = 3), 71.2 μL of PicoGreen working solution, and 100 μL of Tris-EDTA (TE) buffer. The plate was kept in the dark and fluorescence was measured in the microplate reader using an excitation wavelength of 480 nm and an emission wavelength of 528 nm. The dsDNA concentration of each sample was calculated using a standard curve relating DNA concentration and fluorescence intensity.

Total protein quantification. Total protein content was quantified by micro BCA™ assay kit (Pierce Biotechnology, ThermoFisher Scientific). The assay was performed according to manufacturer's instructions. Briefly, standards were prepared at various concentrations ranging from 0 to 200 μg/mL, in ultrapure water. Then, 150 μL of both samples and standards were assayed in triplicate and 150 μL of working reagent was added to each 96-well plate. The plate was sealed and incubated for 2 h at 37°C. Afterward, the plate was left to cool down to RT, and absorbance was read at 562 nm in the microplate reader.

NPs internalization by endothelial and fibroblastic cells. For internalization assays, 5×10^4 HPMECST1.6R and 3×10^4 MRC-5 cells were grown on μ-slides (Ibidi) for confocal microscopy analysis. NPs suspensions previously prepared, as explained above, were added to cultured cells. After 1, 3, and 7 h, cells were fixed with 10% formalin in PBS and stored at 4°C for further staining. Samples were washed three times with PBS and incubated with Triton X-100 0.2% in PBS for 5 min to permeate cell membranes. In the following step, samples were washed with PBS and incubated for 30 min with 3% bovine serum albumin (BSA) in PBS to block non-specific protein interactions. Then, samples were washed with PBS and incubated with phalloidin (0.25 μg/mL) during 15 min to stain cytoskeleton, and with DAPI (1 μg/mL) to label cell nuclei. Images of fluorescent-labeled cells and NPs were obtained by using excitation wavelengths of 405 nm (DAPI), 488 nm (FITC labeled NPs) and 561 nm (phalloidin). Images were acquired using a laser scanning confocal microscopy imaging system (TCS SP8, Leica) at 20× and 63× magnifications.

Statistical analysis

Data from the NPs characterization and biological studies was statistically analyzed using IBM SPSS software (version 21; SPSS Inc.). Shapiro–Wilk test was used to verify the assumption of normality. p values lower than 0.01 were considered statistically significant. Data were analyzed by a non-parametric way by means of a Kruskal–Wallis test followed by Turkey's HSD test.

RESULTS

Size distribution and zeta potential of NPs

PDLA NPs with distinct properties were obtained using different processing conditions. First, the effect of Pluronic® F-68 quantity over NPs size and zeta potential was evaluated. As graphically represented on Figure 1(a1), the surfactant has a huge influence over the size of PDLA NPs. In the absence of Pluronic® F-68, NPs present a significantly higher size than in its presence. The addition of this surfactant leads to a decrease in NPs size in a non-linear trend. In fact, the addition of 12 times the amount of Pluronic® F-68 (0.25 comparing with 3%) leads to NPs with similar sizes. Zeta potentials were all negative, independently of the surfactant amount in the NPs (Fig. 1(b1)). For all formulations, the PDI was lower than 0.1, indicating that NPs have a narrow size distribution. Secondly, the org/aq volume ratio was varied and its influence on the NPs properties previously considered was assessed (Fig. 1(a2, b2)). The overall results of the org/aq volume ratio variation (using a reduced amount of PDLA) showed that NPs size increase as the ratio increases (Fig. 1(a2)). Independently of the org/aq ratio, the values of zeta potentials of NPs were closer to neutrality, but still negative (Fig. 1(b2)). Finally, the presence of the Pluronic® F-68 (0.75%) in this experimental condition was also analyzed. This surfactant led to the formation of polydisperse NPs populations with smaller sizes (81.2 $\pm$ 3.4 nm) and values of zeta potential of −9.15 $\pm$ 6.06 mV.

Based on the previous observations, the conditions 0.25% Pluronic® F-68 and 1:3 org/aq volume ratio without surfactant were selected for further studies and, from now on, designated as types A (120 nm) and B (80 nm) NPs, respectively.

NPs morphology

NPs morphology was evaluated by AFM. The micrographs showed that both types of NPs present a spherical morphology (Fig. 2). Figure 2(a) showed larger NPs than Figure 2(b), corroborating the size measurements assessed by DLS for

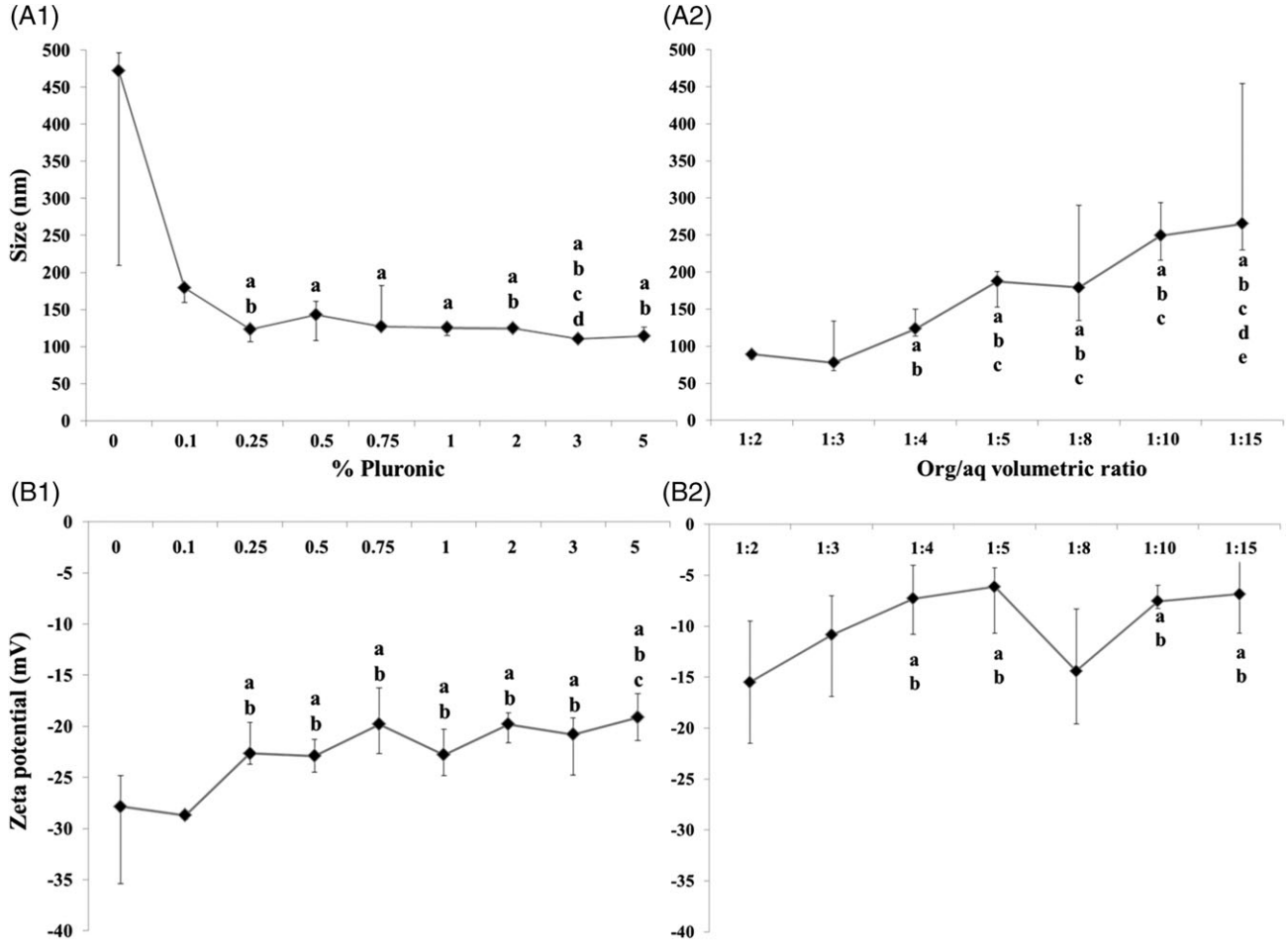

FIGURE 1. Size (A) and zeta-potential (B) of PDLA NPs produced with different percentages of Pluronic® F-68 (**1**) or org/aq volume ratios (**2**). Results represent median (Q2), Q1 and Q3 values. Statistical analysis was performed and data were considered significantly different if $p < 0.01$; (**1**) *a* denotes significant differences compared to 0%, *b* denotes significant differences compared to 0.10%, *c* denotes significant differences compared to 0.50% and *d* denotes significant differences compared to 0.75%; (**2**) *a* denotes significant differences compared to 1:3, *b* denotes significant differences compared to 1:2, *c* denotes significant differences compared to 1:4, *d* denotes significant differences compared to 1:5 and *e* denotes significant differences compared to 1:8.

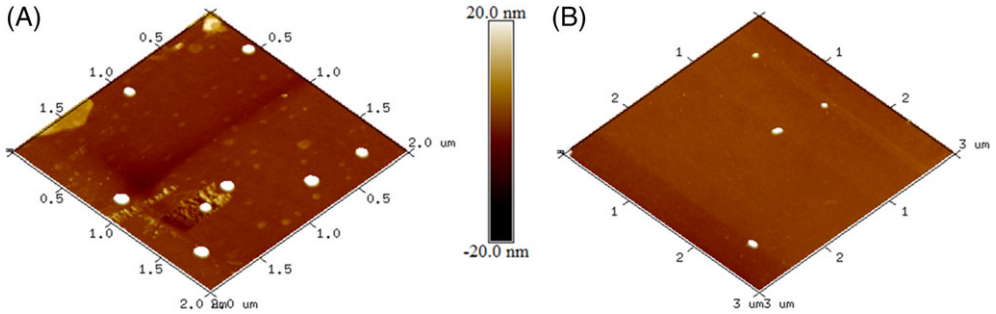

FIGURE 2. AFM microphotographs of the selected PDLA NPs: type A (**a**) and type B (**b**) populations.

types A and B NPs, respectively. A similar conclusion was obtained for NPs size distribution, once it is possible to visualize a more heterogeneous population in Figure 2(b) rather than in Figure 2(a).

Long-term stability

The stability study allowed ensuring the period of time that NPs can be used without an appreciable change of their size, avoiding the occurrence of aggregation and sedimentation in the suspension. Both populations of NPs were kept in water at 4°C, under static conditions. In Figure 3(a) it can be observed that type A NPs kept their size constant during the entire period of time. On the other hand, type B NPs increased their size just 2 weeks after the beginning of the experiment. PDI values of type A NPs kept below 0.1 and for type B NPs they were above 0.2 without a significant change along the time (data not shown). Regarding zeta potential, both NPs populations presented oscillations in the values of this parameter over time (Fig. 3(b)). Sedimentation analysis allowed observing that type B NPs suspensions have a tendency to precipitate over time, contrarily to what was observed for type A NPs.

Drug loading, entrapment efficiency and *in vitro* drug release profile from NPs

Table I presents the results obtained for prednisolone entrapment and loading in type A and type B NPs. It can be observed that type A NPs presented higher values of entrapment efficiency and drug loading than type B NPs.

After quantifying the amount of encapsulated prednisolone, it was evaluated its *in vitro* release profile (Fig. 4). For both types of NPs, the release of prednisolone presented two different phases: first, a burst release and, then, a slight increase in the amount of prednisolone released. It was also possible to observe that type A and type B NPs released 90% of entrapped drug after 24 h and 5 h of the study beginning, respectively.

Biological assays

Human endothelial cells (HPMECST1.6R cell line) were used as a model of vascular endothelium to study NPs uptake. It was also evaluated the ability of NPs to enter in human fibroblastic cells (MRC-5 cell line), since fibroblasts are the most common cells of connective tissues and have an important role in wound healing. Therefore, their cytocompatibility and internalization were assessed to allow concluding about the feasibility of using them in these two biological environments.

NPs cytocompatibility assay. Cell viability (assessed by MTS assay), cell proliferation (assessed by dsDNA quantification; PicoGreen assay) and total protein content (microBCA assay) were determined for human endothelial (Fig. 5) and fibroblastic cells (Fig. 6), cultured during 24, 48, and 72 h with type A or type B NPs.

No substantial differences were observed, in terms of metabolic activity, for both cell types at any time point, and for both types of NPs. Nevertheless, some statistically significant

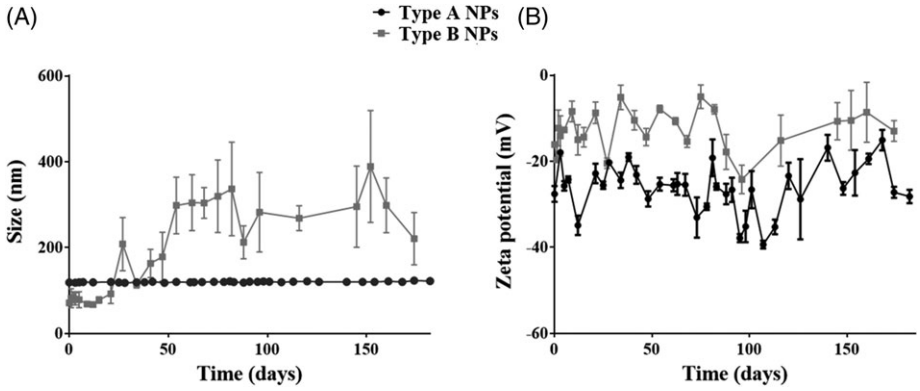

FIGURE 3. Size (**A**) and zeta potential (**B**) of type A (black circles) and type B (gray squares) NPs stored at 4°C in water. Data represent mean ± SD ($n = 3$).

TABLE I. Entrapment efficiency and loading of prednisolone in type A and type B NPs

NPs type	Entrapment efficiency (%)	Drug loading (%)
A	9.69 ± 3.14	32.56 ± 2.76
B	6.13 ± 1.43	14.12 ± 0.86

differences were observed: endothelial cells exposed to NPs suspensions at a concentration of 0.748 mg/mL showed minimal toxicity, especially after 48 h of culture (Fig. 5(a,d)). In terms of dsDNA quantification, for both cell types cultured with both types of NPs, it was possible to observe no statistically significant differences throughout the experiment. Relatively to total protein content, no statistically significant differences were observed for both types of NPs and for both cell types along time. Though, for fibroblastic cells exposed to type A NPs at a concentration of 0.748 mg/mL after 48 h and 72 h, a lower protein concentration was obtained, when compared with the other conditions (Fig. 6(c, f)). Similar results were observed for endothelial cells cultured with type A NPs (Figs. 5(c)).

Nanopartiles internalization. For cells internalization assay, both cell types were exposed during 1, 3, and 7 h to both types of NPs. Their subcellular localization can be observed in Figures 7 and 8. Confocal images showed that fibroblastic cells did not internalize any type of NPs, independently of the time of exposure (Figs. 7(b) and 8(d)). By comparing the micrographs shown in Figure 7(a, c), it is possible to observe that endothelial cells internalized only type A NPs after 3 and 7 h of incubation (Fig. 8). Moreover, cells morphology did not appear to be affected by the presence of NPs (Fig. 7).

DISCUSSION

Herein, the influence of surfactant concentration (i.e., Pluronic® F-68) and the org/aq volume ratio over NPs physical properties was studied. In a further step, and envisioning the use of such NPs in therapeutic applications, an anti-inflammatory drug (i.e., prednisolone) was loaded into the polymeric NPs structure. Both entrapment and loading efficiencies, as well as drug release profile, were evaluated. Considering the future clinical application of NPs, cellular studies (viability, dsDNA, and total protein quantification, as well as cell internalization) were conducted.

Several works in the literature claim that poloxamers (commercially known as Pluronic®) prevent aggregation of NPs.[45] Furthermore, Pluronic® F-68 has the ability to enhance the drug release profile, NPs stability and cell interactions.[46,47] This surfactant can also influence the kinetics of particles clearance. For example, MPs that are usually found in the liver, when coated

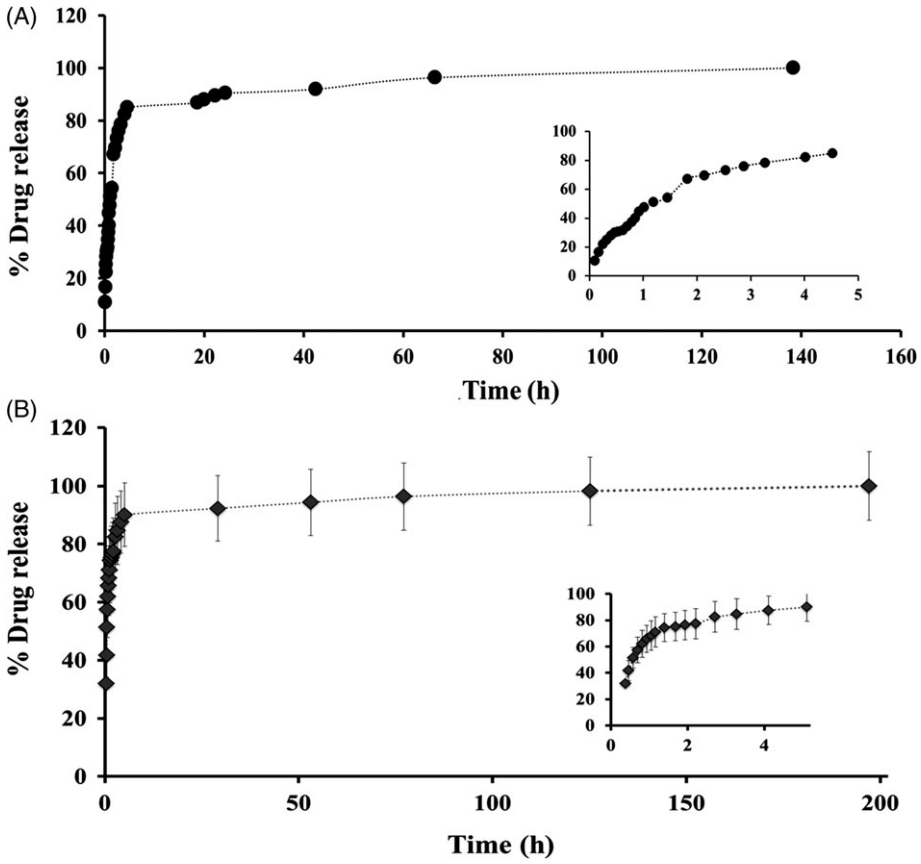

FIGURE 4. Prednisolone release profile from type A (**a**) and type B (**b**) NPs at 37°C. The inset show the release profile over the first 5 h. Data represent mean ± SD (n = 3).

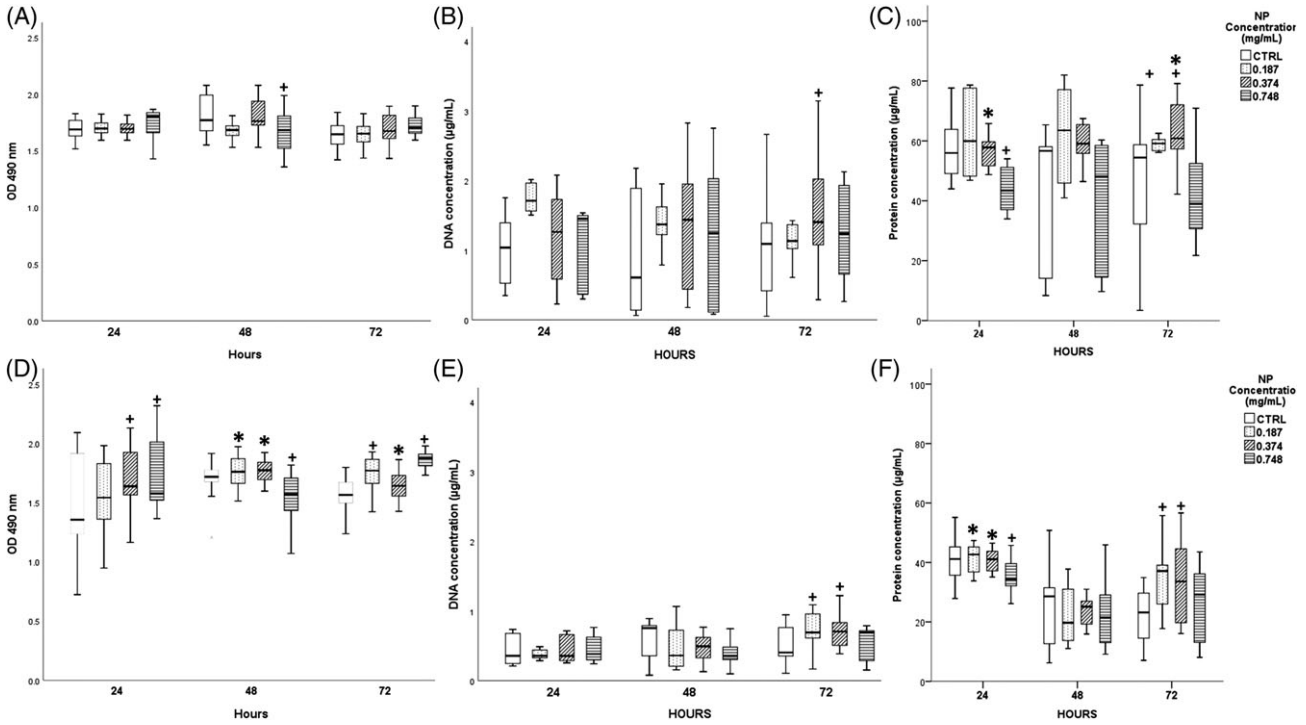

FIGURE 5. Human endothelial cells behavior after exposure to type A NPs suspensions (cells viability [A], dsDNA concentration [B] and total protein content [C]) and to type B NPs suspensions (cells viability [D], dsDNA concentration [E], and total protein content [F]) at different concentrations (0.187 – dotted squares, 0.374 – oblique lines in squares, 0.748 mg/mL – parallel lines in squares, and CTRL – white squares) for each time point (24 h, 48 h, and 72 h). CTRL refers to endothelial cells cultured without NPs. Statistical analysis was performed for all the conditions comparing each concentration for each time point. Data were considered statistically different for $p < 0.01$. + denotes significant differences compared to CTRL, * denotes significant differences compared to concentration 0.748 mg/mL.

with Pluronic® F-68 or Pluronic® F-108 were found in lungs.[48] In fact, coated particles are less covered by opsonins, preventing phagocytic engulfment.[48] Therefore, Pluronic® F-68 was included in the PDLA NPs fabrication method. Experimental data did not allow establishing a linear correlation between the concentration of Pluronic® F-68, NPs size and zeta potential, which might be explained by the presence of different types of interactions between the compounds present in solution. However, we observed that NPs size is significantly smaller for the ones prepared with Pluronic® F-68, but higher amounts of this surfactant did not result in a similar trend in the reduction of NPs size. Indeed, NPs with similar sizes were obtained even after the addition of 12 times the amount of Pluronic® F-68 (0.25 comparing with 3%). In a second approach, different experimental conditions, namely the org/aq volume ratio, were implemented to obtain smaller NPs (inferior to 100 nm). The org/aq volume ratios variation led to NPs whose size values increase as the ratio increases. For all analyzed ratios, the 1:3 ratio was the one that produced smaller NPs.

Two types of NPs with statistically different average sizes (120 nm – type A; 80 nm – type B) were selected. Storage stability assays showed that type A NPs conserved their size during, at least, 6 months at 4°C. At this temperature it is favored the stability of the NPs suspension for longer periods of time. Indeed, it has been described in the literature that lower temperatures of storage ensures a higher chemical stability of the polymers and minimize NPs aggregation.[49,50]

The possibility of NPs aggregation was analyzed by zeta potential, size and PDI determinations over time. Through the analysis of these parameters, it can be concluded that type A NPs did not aggregate or considerably degrade. In accordance, macroscopic sedimentation evaluation did not show the appearance of a precipitate or other visible alteration in the NPs suspension. These results ensure that the NPs can be used without an appreciable change of their characteristics after preparation in the period of time considered. On the other hand, the stability of type B NPs showed to be significantly lower as they rapidly increase in size after the 15th day of storage, keeping constant their polydispersity. This fact is corroborated by Ming et al.[44] that reported an increase of 50 nm on PLGA NPs size after 2 weeks of their preparation. The increase of type B NPs size with time can be due to their smaller zeta potential values (ranging from 0 to −10 mV) and, as a consequence, no strong repulsive forces are present. The instability was also confirmed by the macroscopic sedimentation analysis in which NPs aggregates are present in a higher amount.

The assessment of prednisolone entrapment efficiency and loading, as well as it is *in vitro* release profile, demonstrated that PDLA NPs can be a good carrier for this drug. Although the values of entrapment efficiency and loading are

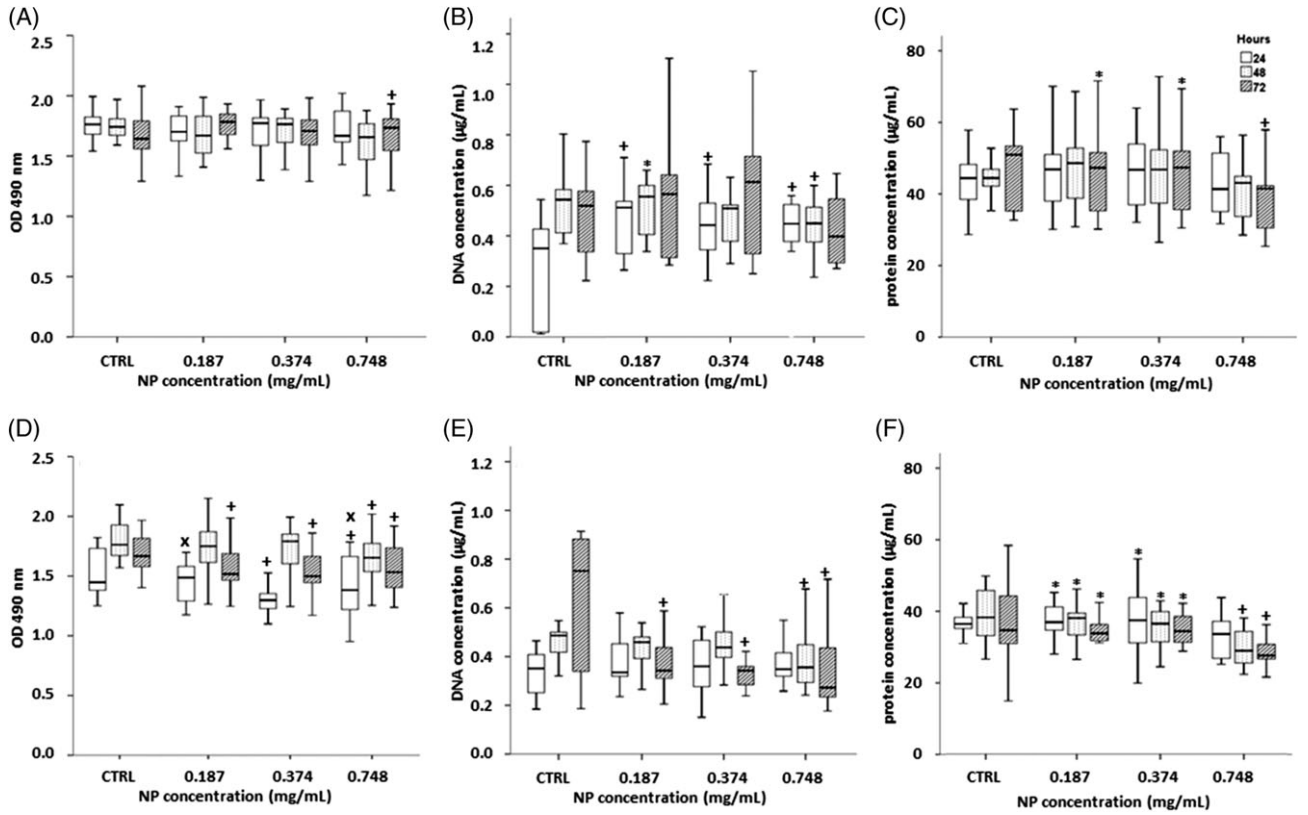

FIGURE 6. Human fibroblastic cells behavior after exposure to type A NPs suspensions (cells viability [A], dsDNA concentration [B] and total protein content [C]) and to type B NPs suspensions (cells viability [D], dsDNA concentration [E], and total protein content [F]) at different concentrations (0.187, 0.374, 0.748 mg/mL and CTRL) for each time point (24 h [white squares], 48 h [dotted squares], and 72 h [striped squares]). CTRL refers to fibroblastic cells cultured without NPs. Statistical analysis was performed for all conditions comparing each concentration for each time point. Data was considered statistically different for $p < 0.01$. + denotes significant differences compared to CTRL, *denotes significant differences compared to concentration 0.748 mg/mL and x denotes significant differences compared to concentration 0.374 mg/mL.

low, it was demonstrated that higher entrapment efficiencies did not imply more entrapped drugs.[51] Indeed, having into consideration the plasma concentration of prednisolone after oral administration,[52] the plasma volume[53] and the mass of the drug incorporated per batch of produced NPs (for example, 177 ± 26 mg for type A NPs), it can be anticipated that the synthetic glucocorticoid is present in an adequate amount to counteract an inflammatory process. Additionally, as prednisolone is incorporated into NPs, it is expected that the plasma concentration will be lower than the obtained with an oral formulation, but higher at the desired local of action.

Prednisolone mode of action is based on its high binding affinity to glucocorticoid receptors that reside in the cytosol.[54] Since this cascade is dependent on the delivery of prednisolone inside the cells to form the steroid/receptor complex, NPs internalization by cells is of major importance. Our experimental data demonstrated that larger NPs (type A NPs) were internalized while smaller (type B NPs) were not, under the experimental conditions used in this work. In fact, while some authors report that the internalization of smaller NPs is higher when comparing to larger NPs,[55,56] others state that there is an ideal NP size for cell internalization to occur.[57,58] Specifically, in the work developed by Win and Feng[58], PLGA NPs with 100 nm were 2.3-fold more internalized than with 50 nm. Despite herein was used PDLA instead of PLGA, our findings are similar to those of Win and Feng.[58]

The biological assays were performed with cell lines presenting a human pulmonary origin but different phenotypes: endothelial (HPMECST1.6R cell line) and fibroblastic (MRC-5 cell line) cells. Fibroblastic cells did not internalize any type of NPs and endothelial cells only internalize 120 nm NPs within our testing conditions. Indeed, there are critical parameters that can influence the internalization of the NPs by cells, such as the size, shape and surface chemistry of the NPs, as well as the target cell.[59] Therefore, among these critical factors, probably the size of the developed NPs is not the ideal to be internalized by human fibroblasts. Indeed, a study performed to evaluate the influence of single-walled carbon nanotubes size in their uptake by fibroblasts also demonstrated that there is a favored size that allows their highest uptake.[60]

The endothelial uptake of circulating NPs is not only fundamental to obtain a localized therapeutic effect, but also to achieve an effective targeting of the NPs in different tissues. The endothelial barrier is composed of a monolayer of endothelial cells with 1 nm tight junctions and 3 nm adherents junctions.[61] Thus, those intercellular spaces are too small for

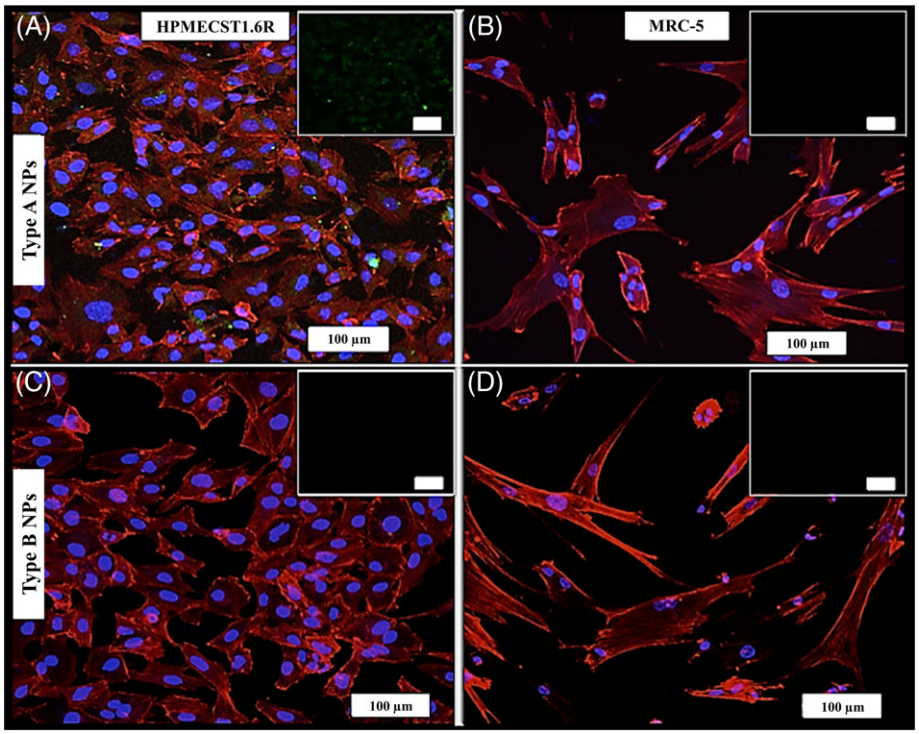

FIGURE 7. Confocal microscopy images of endothelial (A, C) and fibroblastic (B, D) cells cultured during 3 h with 0.748 mg/mL type A (A, B) and type B (C, D) NPs. Cytoskeleton is labeled with phalloidin (in red), nuclei with DAPI (in blue) and NPs, with FITC (in green). Small images show the green channel for a better observation of FITC-NP distribution inside the cellular monolayer.

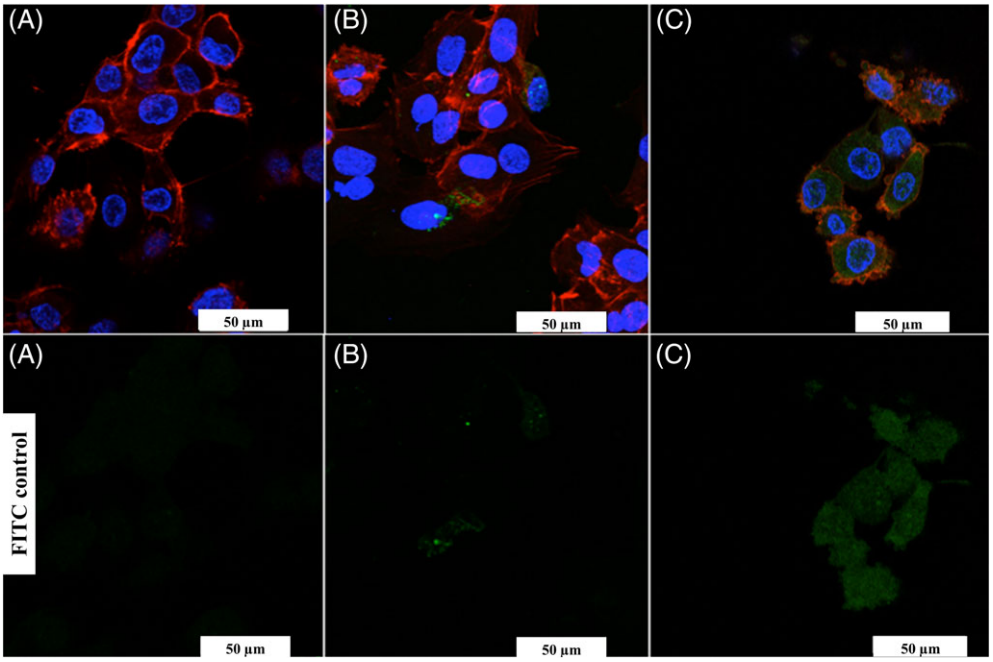

FIGURE 8. Confocal microscopy images of endothelial cells cultured with 0.748 mg/mL type A NPs (in green, FITC), after 1 (A) 3 (B), and 7 h (C), being the nuclei in blue (DAPI) and the cytoskeleton in red (phalloidin). The green channel is shown for a better observation of FITC-NP distribution inside the cellular monolayer.

enabling the extravasation of the NPs. Then, for the NPs to get into the basal side, they should find other alternative paths. The transcellular caveolar pathway, present in endothelial cells of various organs, could provide an alternative intracellular pathway to pass this barrier. Caveolae have ~70 nm in diameter, thus smaller NPs may be preferentially transported by this mechanism than larger NPs.[62,63] However, our experimental results show that only 120 nm NPs

were internalized by human endothelial cells. This result indicates that their intracellular pathway is being used. Consequently, further work is necessary to understand the mechanism regulating the internalization and intracellular pathway of the NPs in the endothelial cells.

CONCLUSIONS

The present study enables concluding that, by adjusting one or more processing parameters of the nanoprecipitation method, it is possible to obtain two statistically different sizes/populations of NPs (i.e., 120 and 80 nm). Their performance as drug delivery systems was validated with the incorporation and sustained release of prednisolone. The developed NPs are cytocompatible as shown in cultures of human endothelial and fibroblastic cells. Furthermore, the two NPs populations presented different internalization profile, depending on NPs size: the endothelial cell line can internalize NPs with 120 nm, whereas fibroblasts did not evidenced internalization of the NPs, independently of their size. The differential internalization profile will be further analyzed in a more in depth study to quantify the internalization of the NPs as well as to study their internalization mechanism by the cells.

In summary, it is possible to conclude that the production of PDLA NPs was successfully optimized to obtain drug delivery devices with promising performance for the treatment of inflammatory diseases.

ACKNOWLEDGMENTS

The authors would like to acknowledge the Portuguese Foundation for Science and Technology for the Post-doc fellowships (SFRH/BPD/90332/2012 and SFRH/BPD/38939/2007), as well as to the QREN (project "RL2 -SCN - NORTE-07-0124-FEDER-000018" co-financed by the North Portugal Regional Operational Program [ON.2, O Novo Norte] under the NSRF through the ERDF) for financing this research work.

CONFLICT OF INTEREST

No benefit of any kind will be received either directly or indirectly by the authors.

REFERENCES

1. Allen TM, Cullis PR. Drug delivery systems: Entering the mainstream. Science 2004;303:1818–1822.
2. Amoozgar Z, Yeo Y. Recent advances in stealth coating of nanoparticle drug delivery systems. Wiley Interdiscip Rev Nanomed Nanobiotechnol 2012;4:219–233.
3. Grabnar PA, Kristl J. The manufacturing techniques of drug-loaded polymeric nanoparticles from preformed polymers. J Microencapsul 2011;28:323–335.
4. Monteiro N, Martins A, Ribeiro D, Faria S, Fonseca NA, Moreira JN, Reis RL, Neves NM. On the use of dexamethasone-loaded liposomes to induce the osteogenic differenciation of human mesenchymal stem cells. J Tissue Eng Regen Med 2013;9:1056–1066.
5. Thambi T, You DG, Han HS, Deepagan VG, Jeon SM, Suh YD, Choi KY, Kim K, Kwon IC, Yi G, Lee JY, Lee DS, Park JH. Bioreducible carboxymethyl dextran nanoparticles for tumor-targeted drug delivery. Adv Healthc Mater 2014;3:1829–1838.
6. Allen TM. Ligand-targeted therapeutics in anticancer therapy. Nat Rev Cancer 2002;2:750–763.
7. Mundargi RC, Babu VR, Rangaswamy V, Patel P, Aminabhavi TM. Nano/micro technologies for delivering macromolecular therapeutics using poly(d,l-lactide-co-glycolide) and its derivatives. J Control Release 2008;125:193–209.
8. Hall JB, Dobrovolskaia MA, Patri AK, McNeil SE. Characterization of nanoparticles for therapeutics. Nanomedicine (Lond) 2007;2:789–803.
9. Ku SH, Kim K, Choi K, Kim SH, Kwon IC. Tumor-targeting multifunctional nanoparticles for siRNA delivery: Recent advances in cancer therapy. Adv Healthc Mater 2014;3:1182–1193.
10. Lockman P, Mumper R, Khan M, Allen D. Nanoparticle technology for drug delivery across the blood-brain barrier. Drug Dev Ind Pharm 2002;28:1–13.
11. Kawaguchi H. Functional polymer microspheres. Prog Polym Sci 2000;25:1171–1210.
12. Hua X, Tan S, Bandara HMHN, Fu Y, Liu S. Externally controlled triggered-release of drug from PLGA micro and nanoparticles. PLoS One 2014;9:1–17.
13. Rizvi SAA, Saleh AM. Applications of nanoparticle systems in drug delivery technology. Saudi Pharm J 2018;26:64–70.
14. Desai MP, Labhasetwar V, Amidon GL, Levy RJ. Gastrointestinal uptake of biodegradable microparticles: Effect of particle size. Pharm Res 1996;13:1838–1845.
15. Ghasemi Y, Peymani P, Afifi S. Quantum dot: Magic nanoparticle for imaging, detection and targeting. Acta Biomed 2009;80:156–165.
16. Ratner BD, Hoffman AS, Schoen FJ, Lemons JE. Biomaterials Science: An Introduction to Materials in Medicine, Third ed. Canada: Academic Press; 2014.
17. Adair JH, Parette MP, Altinoglu EI, Kester M. Nanoparticulate alternatives for drug delivery. ACS Nano 2010;4:4967–4970.
18. Amorim S, Martins A, Neves N, Reis R, Pires R. Hyaluronic acid/-poly-L-lysine bilayered silica nanoparticles enhance the osteogenic differentiation of human mesenchymal stem cells. J Mater Chem B 2014;2:6939–6946.
19. Li L, Yin Q, Cheng J, Lu Y. Polyvalent mesoporous silica nanoparticle-aptamer bioconjugates target breast cancer cells. Adv Funct Mater 2012;1:567–572.
20. Singh R, Lillard J. Nanoparticle-based targeted drug delivery. Exp Mol Pathol 2009;86:215–223.
21. Tzeng SY, Green JJ. Subtle changes to polymer structure and degradation mechanism enable highly effective nanoparticles for siRNA and DNA delivery to human brain cancer. Adv Healthc Mater 2013;2:468–480.
22. Santo VE, Gomes ME, Mano JF, Reis RL. Chitosan-chondroitin sulphate nanoparticles for controlled delivery of platelet lysates in bone regenerative medicine. J Tissue Eng Regen Med 2012;6(Suppl 3):s47–s59.
23. Grenha A, Gomes ME, Rodrigues M, Santo VE, Mano JF, Neves NM, Reis RL. Development of new chitosan/carrageenan nanoparticles for drug delivery applications. J Biomed Mater Res – Part A 2010;92:1265–1272.
24. Vauthier C, Couarraze G. Development of a new drug carrier made from alginate. Am Pharm Assoc 1993;82:912–917.
25. Cui M, Naczynski DJ, Zevon M, Griffi CK, Sheihet L, Poventud-fuentes I, Chen S, Roth CM, Moghe PV. Multifunctional albumin nanoparticles as combination drug carriers for intra-tumoral chemotherapy. Adv Healthc Mater 2013;2:1–10.
26. Harsha S. Pharmaceutical suspension containing both immediate/-sustained-release amoxicillin-loaded gelatin nanoparticles: Preparation and in vitro characterization. Drug Des Devel Ther 2013;7: 1027–1033.
27. Nair LS, Laurencin CT. Biodegradable polymers as biomaterials. Prog Polym Sci 2007;32:762–798.
28. Gilding DK, Reed AM. Biodegradable polymers for use in surgery—Polyglycolic/poly(actic acid) homo- and copolymers. Polymer (Guildf) 1979;20:1459–1464.
29. Hamad K, Kaseem M, Yang HW, Deri F, Ko YG. Properties and medical applications of polylactic acid: A review. Express Polym Lett 2015;9:435–455.
30. Makadia HK, Siegel SJ. Poly lactic-co-glycolic acid (PLGA) as biodegradable controlled drug delivery carrier. Polymer 2011;3:1377–1397.
31. Vogt M, Derendorf H, Kramer J, Junginger HE, Midha KK, Shah VP, Stavchansky S, Dressman JB, Barends DM. Biowaiver monographs for immediate release solid Oral dosage forms: Prednisone. J Pharm Sci 2007;96:1480–1489.

32. Wassenberg S, Rau R, Steinfeld P, Zeidler H. Very low-dose prednisolone in early rheumatoid arthritis retards radiographic progression over two years: A multicenter, double-blind, placebo-controlled trial. Arthritis Rheum 2005;52:3371–3380.
33. Kavanaugh A, Wells AF. Benefits and risks of low-dose glucocorticoid treatment in the patient with rheumatoid arthritis. Rheumatol (Oxford) 2014;53:1742–1751.
34. Neves J, Michiels J, Ariën KK, Vanham G, Amiji M, Bahia MF, Sarmento B. Polymeric nanoparticles affect the intracellular delivery, antiretroviral activity and cytotoxicity of the microbicide drug candidate dapivirine. Pharm Res 2012;29:1468–1484.
35. Clemens DL, Lee B, Xue M, Thomas CR, Meng H, Ferris D, Nel AE, Zink JI, Horwitz MA. Targeted intracellular delivery of antituberculosis drugs to mycobacterium tuberculosis-infected macrophages via functionalized mesoporous silica nanoparticles. Antimicrob Agents Chemother 2012;56:2535–2545.
36. Paulo CSO, Pires R, Ferreira LS. Nanoparticles for intracellular-targeted drug delivery. Nanotechnology 2011;22:1–11.
37. Ghosh P, Yang X, Arvizo R, Zhu Z, Agasti SS. Intracellular delivery of a membrane-impermeable enzyme in active form using functionalized gold nanoparticles. J Am Chem Soc 2011;132:2642–2645.
38. Yameen B, Choi WI, Vilos C, Swami A, Shi J. Insight into nanoparticle cellular uptake and intracellular targeting. J Control Release 2014;190:485–499.
39. Nobs L, Buchegger F, Gurny R, Allémann E. Poly(lactic acid) nanoparticles labeled with biologically active Neutravidin™ for active targeting. Eur J Pharm Biopharm 2004;58:483–490.
40. Nobs L, Buchegger F, Gurny R, Alle E. Biodegradable nanoparticles for direct or two-step tumor immunotargeting. Bioconjug Chem 2006;17:139–145.
41. Howard MD, Hood ED, Greineder CF, Alferiev IS, Chorny M, Muzykantov V. Targeting to Endothelial Cells Augments the Protective Effect of Novel Dual Bioactive Antioxidant/Anti-Inflammatory Nanoparticles. Mol. Pharmaceutics 2014;11:2262–2270.
42. Flavell SJ, Hou TZ, Lax S, Filer AD, Salmon M, Buckley CD. Fibroblasts as novel therapeutic targets in chronic inflammation. Br J Pharmacol 2008;153:241–246.
43. Paiva AM, Pinto RA, Teixeira M, Barbosa CM, Lima RT, Vasconcelos MH, Sousa E, Pinto M. Development of noncytotoxic PLGA nanoparticles to improve the effect of a new inhibitor of p53–MDM2 interaction. Int J Pharm 2013;454:394–402.
44. Hu C-MJ, Zhang L, Aryal S, Cheung C, Fang RH, Zhang L. Erythrocyte membrane-camouflaged polymeric nanoparticles as a biomimetic delivery platform. Proc Natl Acad Sci U S A 2011;108:10980–10985.
45. Jain D, Athawale R, Bajaj A, Shrikhande S, Goel PN, Gude RP. Studies on stabilization mechanism and stealth effect of poloxamer 188 onto PLGA nanoparticles. Colloids Surf. B Biointerf 2013;109:59–67.
46. Santander-Ortega MJ, Jódar-Reyes AB, Csaba N, Bastos-González D, Ortega-Vinuesa JL. Colloidal stability of Pluronic F68-coated PLGA nanoparticles: A variety of stabilisation mechanisms. J Colloid Interface Sci 2006;302:522–529.
47. Csaba N, González L, Sánchez A, Alonso MJ. Design and characterisation of new nanoparticulate polymer blends for drug delivery. J Biomater Sci Polym Edn 2004;15:1137–1151.
48. Tabata Y, Ikada Y. Phagocytosis of polymer microspheres by macrophages. Adv Polym Sci 1990;94:107–141.
49. Abdelwahed W, Degobert G, Stainmesse S, Fessi H. Freeze-drying of nanoparticles: formulation, process and storage considerations. Adv Drug Deliv Rev 2006;58:1688–1713.
50. Coffin M, McGinity J. Biodegradable pseudolatexes: the chemical stability of poly (D,L-lactide) and poly (ε-caprolactone) nanoparticles in aqueous media. Pharm Res 1991;9:200–205.
51. Ferreira H, Silva R, Matamá T, Silva C, Gomes AC, Cavaco-Paulo A. A biologically active delivery material with dried-rehydrated vesicles containing the antiinflammatory diclofenac for potential wound healing. J Liposome Res 2016;26:269–275.
52. Wilson CG, May CS, Paterson JW. Plasma prednisolone levels in man following administration in plain and enteric-coated forms. Br J Clin Pharmac 1977;4:351–355.
53. Hurley PJ. Red cell and plasma volumes in normal adults. J Nucl Med 1975;16:46–52.
54. Frijters R, Fleuren W, Toonen E, Tuckermann J, Reichardt H, Maaden H, Elsas A, Lierop M-J, Dokter W, Vlieg J, Alkema W. Prednisolone-induced differential gene expression in mouse liver carrying wild type or a dimerization-defective glucocorticoid receptor. BMC Genomics 2010;11:359.
55. Zauner W, Farrow NA, Haines AMR. In vitro uptake of polystyrene microspheres: Effect of particle size, cell line and cell density. J Control Release 2001;71:39–51.
56. Oh E, Delehanty JB, Sapsford KE, Susumu K, Goswami R, Blanco-Canosa J, Dawson P, Granek J, Shoff M, Zhang Q, Goering P, Huston A, Medintz I. Cellular uptake and fate of PEGylated gold nanoparticles is dependent on both cell-penetration peptides and particle size. ACS Nano 2011;5:6434–6448.
57. Kulkarni SA, Feng S-S. Effects of particle size and surface modification on cellular uptake and biodistribution of polymeric nanoparticles for drug delivery. Pharm Res 2013;30:2512–2522.
58. Win KY, Feng S-S. Effects of particle size and surface coating on cellular uptake of polymeric nanoparticles for oral delivery of anticancer drugs. Biomaterials 2005;26:2713–2722.
59. Oh N, Park JH. Endocytosis and exocytosis of nanoparticles in mammalian cells. Int J Nanomedicine 2014;9:51–63.
60. Jin H, Heller DA, Sharma R, Strano MS. Size-dependent cellular uptake and expulsion of single-walled carbon nanotubes: single particle tracking and a generic uptake model for nanoparticles. ACS Nano 2009;3:149–158.
61. Yuan S, Rigor R. Regulation of Endothelial Barrier Function. San Rafael: Morgan & Claypool Life Sciences; 2011.
62. Wang Z, Malik AB. Nanoparticles squeezing across the blood–endothelial barrier via caveolae. Ther Deliv 2013;4:131–133.
63. Komarova Y, Malik AB. Regulation of endothelial permeability via paracellular and transcellular transport pathways. Annu Rev Physiol 2010;72:463–493.